frontiers | Frontiers in Nanotechnology

TYPE Original Research
PUBLISHED 17 July 2024
DOI 10.3389/fnano.2024.1419239



OPEN ACCESS

EDITED BY
Aylin Marz,
Norfolk State University, United States

REVIEWED BY
Pramod K. Gupta,
Fraunhofer USA (FHG), United States
Snehasis Bhakta,
Cooch Behar College, India

*CORRESPONDENCE
J. A. Zamora-Justo,
jzamoraj@ipn.mx

RECEIVED 17 April 2024
ACCEPTED 12 June 2024
PUBLISHED 17 July 2024

CITATION
Santos-Santos IJ, Zamora-Justo JA, Vázquez-Martínez GR, Cabrera-Sierra R and Balderas-López JA (2024), Synthesis of gold nanoparticles coated with glucose oxidase using PVP as passive adsorption linkage. *Front. Nanotechnol.* 6:1419239. doi: 10.3389/fnano.2024.1419239



# Synthesis of gold nanoparticles coated with glucose oxidase using PVP as passive adsorption linkage

I. J. Santos-Santos[1], J. A. Zamora-Justo[2]*, G. R. Vázquez-Martínez[3], R. Cabrera-Sierra[1] and J. A. Balderas-López[2]

[1]Instituto Politécnico Nacional, Escuela Superior de Ingeniería Química e Industrias Extractivas, Department of Industrial Chemical Engineering, Mexico City, Mexico, [2]Instituto Politécnico Nacional, Unidad Profesional Interdisciplinaria de Biotecnología, Basic Sciences Department, Mexico City, Mexico, [3]Universidad Tecnológica de México (UNITEC), Campus Cuitláhuac, Department of Chemical Engineering, Mexico City, Mexico

Gold nanoparticles (AuNPs) have great potential as biosensors for glucose detection due to their high sensitivity, as well as their extraordinary physical and chemical properties that improve compatibility with different biorecognition molecules, such as glucose oxidase (GOx). In this work the D-glucose quantification was determined by using the traditional technique based on biochemical reaction of GOx and AuNPs functionalized with polyvinylpirrolidone (PVP) polymer and the enzyme. The AuNPs-PVP-GOx nanocomplexes were characterized by ultraviolet-visible (UV-Visible), Infrared (FTIR), and Raman spectroscopies, as well as scanning electron microscopy (SEM), Z potential, dynamic light scattering (DLS), and thermogravimetry analysis (TGA). In general, these techniques showed significant differences after each functionalization stage with PVP and GOx, for instance it was observed: the presence of different functional groups, an increase of hydrodynamic diameter from 48.60 to 198.77 nm, a shift of the band absorption to larger wavelength, a change in the surface potential and weight loss, and in the morphology of the nanocomplex, which confirm the functionalization. In addition, the enzymatic activity of the AuNPs-PVP-GOx was confirmed through the detection of triiodide ions by UV-Visible spectrophotometry, coming from the oxidation reaction of iodide ions in the presence of $H_2O_2$. Furthermore, the nanocomplex synthesized by passive adsorption was evaluated as a possible biosensor for the quantification of D-glucose using a colorimetric assay, obtaining greater sensitivity than the

**Abbreviations:** AuNPs, Gold nanoparticles; AuNPs-PVP, Gold nanoparticles with Polyvinylpyrrolidone; AuNPs-PVP-GOx, Gold nanoparticles with Polyvinylpyrrolidone and glucose oxidase; GOx, Glucose Oxidase; DLS, Dynamic Light Scattering; DSP, Disodium phosphate; EDC, N-ethyl-N′-(3-dimethylaminopropyl) carbodiimide; EDS, Energy-Dispersive X-ray Spectrometry; IR Infrared Spectrometry; LOD, Limit of detection; NPs, Nanoparticles; NHS, N-hydroxysuccinimide; MKP, Monopotassium phosphate; PAA, Polyacrylic acid PBS, Phosphate buffer; PDDA Poly (diallyldimethylammonium chloride) PEI, Polyethylenimine; PEG, Polyethylene Glycol; PSS, Poly (4-styrenesulfonic) acid; PVA, Polyvinyl alcohol; PVP, Polyvinylpyrrolidone; SEM, Scanning Electron Microscopy; SPR, Surface Resonance Plasmon; TGA, Thermogavimetric Analysis.

traditional method. These findings indicate that PVP can be used as a linkage medium between AuNPs and GOx, which in turn can be used as a biosensor for the detection of D-glucose at low concentrations in biological fluids.

KEYWORDS

gold nanoparticles, D-glucose, glucose oxidase, polyvinylpyrrolidone, biosensor

# 1 Introduction

Gold nanoparticles (AuNPs) have attracted great interest in the scientific community in the last decades, due to their physical (e.g., their characteristic surface plasmon resonance, SPR) and chemical properties that make possible their functionalization with a variety of ligands (Nooranian et al., 2021). Biosensors based on aptamer-conjugated gold nanoparticles: A review. Biotechnology and Applied Biochemistry (Aldewachi et al., 2018; Sarfraz and Khan, 2021).

AuNPs have been used in different scientific areas, especially in the biomedical field (Yeh et al., 2012; Bansal et al., 2020) since they are useful for detection or quantification of some analytes in real time (Aldewachi et al., 2018; Nukaly and Ansari, 2023), for instance, they could be used as biosensor to quantify the glucose concentration in blood (Aldewachi et al., 2018; Pullano SA et al., 2022) and they can be commercially exploited as a regular test for people with diabetes (Shoaib et al., 2023).

In general, biosensors are devices which have the purpose of detect and quantify a specific analyte of biochemical interest (Naresh and Lee, 2021) and they can be classified into the following categories: electrochemical, optical, thermometric, piezoelectric, and magnetic (Naresh and Lee, 2021). Some common optical biosensors for glucose quantification are based on colorimetric assays that use the reaction between a specific enzyme and the analyte to produce a color change (Xin Ting Zhao et al., 2019; Si et al., 2021). It has been shown that the use of AuNPs as substrate for optical biosensor can be useful to improve the color intensity of the assays and increase the sensitivity of the devices (Aldewachi et al., 2018). However, it is necessary to select a specific biorecognition molecule and bind it on the gold nanoparticles surface, for instance Alshanberi et al. (Alshanberi et al., 2021) linked galactosidase to the AuNPs' surface, enhancing its enzymatic activity.

Glucose oxidase (GOx) is the most used biomolecule for D-glucose oxidation and quantification (Bauer JA et al., 2022). This process is represented by the following biochemical reaction:

$$\text{Glucose} + H_2O \xrightarrow{\text{GOx}} \text{Gluconic acid} + H_2O_2 \quad (1)$$

In this oxidation reaction, hydrogen peroxide and D-glucono-δ-lactone are produced; the latter spontaneously hydrolyzes to gluconic acid using molecular oxygen as an electron receptor (Bankar et al., 2009).

Recently, several methods for enzyme immobilization on AuNPs' surface have been reported (Lipińska et al., 2021). Chemical immobilization methods consist of the formation of direct covalent bonds between terminal functional groups of the enzyme and AuNPs (Moses Phir et al., 2019). Some examples of this type of functionalization are the use of Polyethylene Glycol (PEG) (Zamora-Justo et al., 2019; Amina and Guo, 2020), N-ethyl-N'-(3-dimethylaminopropyl) carbodiimide (EDC), and N-hydroxysuccinimide (NHS) (Li et al., 2007; Yang et al., 2019), and some amino acids (Moses Phir et al., 2019). Dongxiang et al. (Li et al., 2007) synthesized AuNPs using sodium citrate; these AuNPs were functionalized with a thiol group with COOH endings and were subsequently linked with amino groups on the protein surface by activating the carboxyl groups with EDC/NHS. Additionally, Moses et al., (Moses Phiri et al., 2019), modified AuNPs using L-cysteine and subsequently covalently linked them to NHS-activated GOx to fabricate a stable and sensitive bioconjugate complex. From these works, it becomes evident that the reported methodology can be complex due to the number of processes and chemical reagents that are required for the functionalization of AuNPs with GOx.

On the other hand, physical methods consist of the passive adsorption of atoms or molecules on the nanoparticle surface due to Van der Waals forces (Aldewachi et al., 2018). However, the disadvantages of this method are that the bond may not be stable and permanent, for this reason a decrease in the enzymatic activity can be expected (Moses Phiri et al., 2019). However, these disadvantages can be improved by using polymers which provide greater stability and binding to other molecules, (Dhumale et al., 2012; Xu et al., 2022). The functionalization with polymers has various advantages over chemical methods since it is faster, simpler, cheaper, and does not require great quantities of chemical reagents (Putzbach and Ronkainen, 2013; Goossens et al., 2017; Moses Phiri et al., 2019). An example of this functionalization is the work of Alshanberi et al. (Alshanberi et al., 2021) in which AuNPs were synthesized by modifying their surface with polyvinyl alcohol (PVA) and linking it to the β-galactosidase enzyme. The advantages of coating AuNPs with polymers are greater stability, high surface density, and the ability to adjust AuNPs' solubility (Mahato et al., 2019). Polymers that have been used as linkage include polyacrylic acid (PAA) (Arkaban H et al., 2022), polyvinyl alcohol (PVA) (Liu B et al., 2022), polyethylenimine (PEI) (Fahira A et al., 2022), poly (diallyldimethylammonium chloride) (PDDA) (Zhou et al., 2019), and poly (4-styrenesulfonic) acid (PSS) (Xu et al., 2022). Particularly, the use of polyvinylpirrolidone (PVP) as a coating agent has improved the AuNPs stability avoiding their aggregation (Mohamed et al., 2017); enzyme adsorption is also favored due to its excellent biocompatibility, which is a useful feature to encapsulate drugs in the pharmaceutic industry (Teodorescu and Bercea, 2015). In addition, Dhumale et al. (Dhumale et al., 2012) synthesized PVP coated AuNPs, and it was shown that the particle aggregation increased as the pH in the colloidal systems decreased. Although there are several reports on the use of AuNPs and PVP, so far PVP has not been used as a linkage agent for GOx.

In this work gold nanoparticles were synthesized and coated with PVP polymer and functionalized with GOx by passive adsorption method; these nanocomplexes have showed potential for the development of new non invasives biosensors with higher

sensitivity and selectivity, than traditional ones (Nooranian et al., 2021). Other advantages to highlight are that they do not generate skin irritation, tissue composition interference (Peng et al., 2022) and have a lower cost. In addition, the development of this biosensor has a longer useful life compared to commercial glucometers (14 days) and the cost that the user must constantly pay is $100.00 USD or more (Johnston L et al., 2021). Furthermore, the advantage of using biosensors based on AuNPs functionalized with polymers and GOx is that this biorecognition molecule can be fixed in paper microfluidics or forming films based on polymers (electrospum) (Sapountzi et al., 2017), whose useful life is longer due to their excellent stability provided by polymers.

This is a very important matter since the development of non-invasive glucose biosensors is based on the quantification of this carbohydrate in biofluids like urine, tears, sweat, and saliva (Pullano SA et al., 2022; Reddy et al., 2022); especially because, according to Johnston et al. (Johnston et al., 2021), the concentration of glucose in these biofluids is up to 50 times lower than that of blood.

The quantification of D-glucose in glucose solutions with concentrations in the range of saliva was performed by using UV-Vis spectrophotometry; for this, it was implemented a biosensor based on AuNPs functionalized with PVP and GOx since at low concentrations the conventional enzymatic method with GOx is not sensitive. In our functionalization method, the polymer was added on the surface of the nanoparticles (passive adsorption); due to physicochemical properties of PVP, complexes or matrices were formed (Franco and De Macro, 2020). GOx molecules were thus trapped, carrying out the functionalization while providing nanocomplexes with greater stability and without loss of enzymatic activity. The resulting nanocomplexes were characterized by UV-Visible, infrared (IR), Raman, and Z potential spectroscopies, dynamic light scattering (DLS), thermogravimetry analysis (TGA), and SEM images coupled to energy-dispersive X-ray spectrometry (EDS). It is worth to mention at this sense that there were differences in the results of each technique which confirm the functionalization.

Furthermore, the biological activity of the nanocomplexes was evaluated using two colorimetric tests; the first was carried out to confirm the presence of GOx, and the second test was to evaluate its enzymatic activity using low concentrations of glucose that resemble those of biofluids (e.g., as saliva) (Johnston et al., 2021).

# 2 Materials and methods

## 2.1 Materials

Tetrachloroauric acid trihydrate or gold salt ($HAuCl_4.3H_2O$), sodium citrate ($Na_3C_6H_5O_7$), phosphate buffer (PBS), polyvinylpyrrolidone (PVP), ammonium molybdate ($(NH_4)_6Mo_7O_{24}$), sucrose, mannose, D-fructose, agarose, D-glucose, and glucose oxidase (GOx) (EC.1.1.3.4, 176 u/g solid) from *Aspergillus niger*, were purchased from Sigma-Aldrich. Hydrochloric acid (HCl), potassium iodide (KI), and hydrogen peroxide ($H_2O_2$), sodium chloride (NaCl, 137 mmol/L), potassium chloride (KCl, 2.7 mmol/L), disodium phosphate (DSP) ($Na_2HPO_4$, 10 mmol/L) and monopotassium phosphate (MKP) ($KH_2PO_4$, 1.8 mmol/L), were purchased from FERMONT, Mexico. All glassware was washed with aqua regia before their use. All the solutions were prepared using deionized water from a Millipore Milli-Q purificator.

## 2.2 Synthesis of gold nanoparticles

AuNPs were synthesized using the Turkevich method (Kimling et al., 2006). 500 µL of 1% tetrachloroauric acid solution were poured into 50 mL of Milli-Q water and the mixture was heated until boiling. After this, 10 mL of 1% sodium citrate solution was slowly added. The reaction turned to a red wine color after 30 min, which confirms the synthesis of gold nanoparticles.

## 2.3 Functionalization of AuNPs with PVP and GOx

AuNPs were functionalized with PVP and GOx based on passive adsorption. 50 mL of the AuNPs solution was centrifuged at 10,000 rpm for 10 min. The precipitate was diluted in 50 mL of 4% PVP solution and the mixture was rotated for 12 h in a shaker flask at 200 rpm (Dhumale et al., 2012). The resulting solution (labeled as AuNPs-PVP) was then centrifuged three times under the same conditions, and resuspended in PBS (10 mM, pH 7). For functionalization with GOx, 30 mL of AuNPs-PVP were mixed with 20 mL of GOx (2,000 units). The mixture was poured into a flask shaker and rotated at 200 rpm for 12 h at room temperature. The resulting nanocomplexes were centrifuged and washed three times with PBS under the same conditions. Finally, the modified nanoparticles (labeled as AuNPs-PVP-GOx) were resuspended in PBS and stored at 4°C until use. It is worth to mention that the AuNPs and nanocomplexes were sonicated before any characterization for 20 min in the ultrasonic cleaner AS3120B at 40 kHz to avoid agglomerations.

## 2.4 Characterization of the gold nanoparticles

To distinguish between the functional groups of the PVP and GOx molecules that were linked to the AuNPs' surface, infrared (IR) and Raman characterizations were performed. KBr tablets were prepared according to Meyer's method (Meyer et al., 2004), by transferring to a stainless-steel matrix of 13 mm diameter and pressed for 30 s with a Specac press under a force of 8 tons. Likewise, KBr modified tablets were prepared by mixing 10 mg powder (high purity PVP and GOx) with KBr. In both cases, KBr can be used for analyzing organic and inorganic compounds because it does not absorb IR radiation. For synthesis and functionalization, gold nanoparticles were poured for 48 h on the KBr pellets and set in a desiccator to dry before their characterization. After the preparation of the samples, infrared spectra were recorded in the spectral range of 4,000–650 $cm^{-1}$ by using a Perkin Elmer, Spectrum RX I FT-IR system.

On the other hand, the Raman measurements were performed using a Horiba Jobin Yvon micro-Raman spectroscope model

TABLE 1 Composition of each sample for colorimetric assays.

| Sample | D-glucose solution (μL) | Glucose oxidase (μL) | AuNPs (μL) | AuNPs-PVP (μL) | AuNPs-PVP-GOx (μL) | Carrier solution (μL) |
|---|---|---|---|---|---|---|
| Glucose oxidase (positive control) | 300 | 300 | - | - | - | 300 |
| AuNPs | 300 | - | 300 | - | - | 300 |
| AuNPs-PVP | 300 | - | - | 300 | - | 300 |
| AuNPs-PVP-GOx | 300 | - | - | - | 300 | 300 |

HR800, with an excitation laser set at 785 nm, with a nominal power of 36.3 mW, and a multi-channel detector CCD Synapse.

Furthermore, the thermal stability of the materials as a function of the temperature was studied by thermogravimetric analysis (TGA) using a Thermal Analyzer STA 6000. These measurements were performed using 100 μL of each sample with a temperature ramp of 30°C–500°C at a heating rate of 8°C per minute.

The nanoparticles size and the morphology of the synthesized AuNPs were analyzed by scanning electron microscopy (SEM); 100 μL of AuNPs, AuNPs-PVP, and AuNPs-PVP-GOx with a concentration of 3 μg/mL were separately dried on aluminum surface and analyzed using a Field Emission Scanning Electron Microscope JSM-7800F, equipped with an EDS EDAX detector. In addition, the EDS spectra were recorded to identify which chemical elements were present in the samples.

The characterization of AuNPs, AuNPs-PVP, and AuNPs-PVP-GOx was carried out by ultraviolet-visible spectrophotometry using the PBS buffer solution as a blank. Spectra were recorded from 190 to 750 nm, with a scanning rate of 60 nm per minute using a Perkin Elmer spectrometer Lambda 2S. The hydrodynamic diameter of the nanoparticles and the electric potential (*Z* potential) on the nanocomplexes surface were measured by DLS using a Malvern Zetasizer Nano *Z*, diluting the samples 1:1000 in PBS.

## 2.5 Colorimetric assay

To verify the presence of GOx on AuNPs' surface, its biological activity was evaluated at each functionalization stage using a colorimetric assay; these results were compared with those obtained in the presence of GOx as a positive control.

The carrier solution was prepared by dissolving 0.8306 g of potassium iodide and 0.0125 g of ammonium molybdate in 250 mL of PBS. 300 μL of this solution was mixed into a flask with 300 μL of D-glucose (200 mg/dL) and 300 μL of GOx, or nanocomplex solution, as indicated in Table 1; the following reaction was carried out for 1 h:

$$\begin{aligned} \text{Glucose} + H_2O &\xrightarrow{\text{GOx}} \text{Gluconic acid} + H_2O_2 \\ H_2O_2 + I^- &\rightleftarrows I_2 \\ I_2 + I^- &\rightleftarrows I_3^- \end{aligned} \tag{2}$$

Glucose was oxidized by GOx to produce gluconic acid and hydrogen peroxide which reacts with iodide ions forming iodine and/or triiodide ions. This complex shows a yellow color shade whose intensity is proportional to the concentration of glucose and/or triiodide ions formed during the reaction (Li et al., 2017).

## 2.6 UV-vis characterization of triiodide ions

The formation of triiodide ions ($I_3^-$) takes place according to Eq. 2 and it absorbs electromagnetic radiation in the UV-Vis region (Afrooz and Dehghani, 2015). Two absorption bands at 280 and 360 nm have been reported (Afrooz and Dehghani, 2015), which can be used to identify their formation. To confirm the presence of these ions, the reaction was carried out with different standards of hydrogen peroxide and potassium iodide for 5 minutes and characterized by UV-Visible spectroscopy.

A stock solution of 250 mg/L of $H_2O_2$ was prepared using a 30% hydrogen peroxide solution dissolved in Mili-Q water. From this solution, different standards (0.5, 1, 2.5, 5, 7.5, and 10 ppm) were prepared; thereafter, each standard was reacted with potassium iodide solutions (carrier solution) for 5 min to obtain the triiodide ions, which were further characterized by UV-Visible spectroscopy. The reaction was carried out by mixing peroxide and carrier solutions at a 1:1 volume ratio.

## 2.7 Enzymatic assay with glucose oxidase and AuNPs-PVP-GOx

Three different solutions of D-glucose were prepared with concentrations within the range of saliva (1 mg/dL, 10 mg/dL, and 20 mg/dL) (Reddy et al., 2022). Two types of experiments were performed: 1) D-glucose solutions were reacted with pure GOx for 5 min and characterized by UV-Visible spectrometry, 2) to confirm the enzymatic activity of functionalized AuNPs, the enzymatic assay was performed by using synthesized AuNPs-PVP-GOx with the same D-glucose concentrations. Notice that in this experiment GOx was not added to the reactions to demonstrate the enzymatic activity of the functionalized nanoparticles. The same characterization by UV-Visible spectroscopy was performed after 5 min and 2.5 h of reaction, using the mixture of distilled water, GOx, and carrier solution as a blank. This test was performed in triplicate to ensure repeatability.

## 2.8 Selectivity test

A selectivity test was carried out to determine if the nanocomplexes (AuNPs-PVP-GOx) can react with other carbohydrates which can be found in foods or in some biological biofluids, especially in saliva. For this test, solutions of D-glucose, sucrose, mannose, D-fructose, and agarose were prepared at 60 mg/

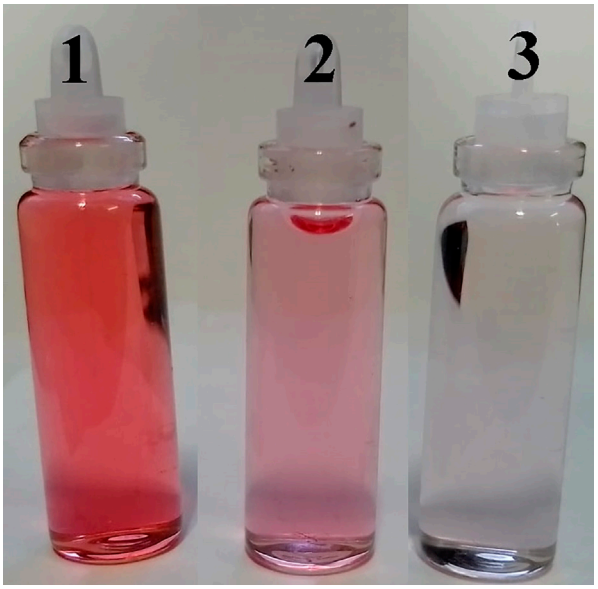


FIGURE 1
Colloids obtained after the synthesis and functionalization process (a) 1) AuNPs; 2) AuNPs-PVP; and 3) AuNPs-PVP-GOx.

dL. Each of these biomolecules was then reacted with the nanocomplexes and potassium iodide; after 5 min, the same UV - visible characterization was recorded to detect the likely formation of triiodide ions due to the enzymatic activity of GOx present on the nanoparticles surface.

# 3 Results

## 3.1 AuNPs

AuNPs were synthesized following the method described by Turkevich (Kimling et al., 2006) and functionalized with PVP and GOx by the passive adsorption method (Alshanberi et al., 2021). Homogeneous colloids were obtained from each sample and without precipitates (Figure 1). The AuNPs solution showed a characteristic wine-red color (Figure 1, sample 1). In the case of AuNPs-PVP, a pink color was evident (Figure 1, sample 2) and finally AuNPs-PVP-GOx, which showed a clear pink color (Figure 1, sample 3).

## 3.2 IR analysis

For comparison purposes, the infrared (IR) spectra of PVP and GOx were obtained and shown in Figure 2 to identify their characteristic functional groups in the functionalization of AuNPs. The peaks around 1400 $cm^{-1}$ and 1600 $cm^{-1}$ (Figure 2A, black line) are related to symmetric and asymmetric stretching of the C=O bond from the sodium citrate ions remaining on the gold nanoparticles' surface (Shahbazi and Zare-Dorabei, 2019). The signal at 1400 $cm^{-1}$ was stronger for the AuNPs-PVP nanocomplexes (Figure 2B) since it is due to the CH deformation modes of the $CH_2$ group (Abdelghany et al., 2023). Furthermore, a bending vibration at 1291 $cm^{-1}$ is observed, which is attributed to the C-N bond of the pyrrolidone structure (Abdelghany et al., 2023), confirming the functionalization of AuNPs with PVP. Additionally, the absorption band around 3,125 $cm^{-1}$ is attributed to the O-H bonds of the sodium citrate ions; and the likely intermolecular hydrogen bonding (Aldewachi et al., 2018). Figure 2C shows a comparison between the IR spectra of GOx and the AuNPs-PVP-GOx nanocomplexes. Peaks at 1652 $cm^{-1}$ and 1539 $cm^{-1}$ for the GOx spectrum correspond to amide II (C=O) and amide I (N-H and C-H) groups (Chey et al., 2012; Abdelghany et al., 2023), respectively. The peak at 1400 $cm^{-1}$ is attributed to the presence of carboxyl groups. The signals of the amide II and carboxyl groups were also identified in AuNPs-PVP-GOx nanocomplexes (Figures 2A, C), suggesting that PVP and GOx are indeed attached to the AuNPs. However, there is an evident decrease in the intensity of the peak at 1400 $cm^{-1}$ which is attributed to a shield effect due to the larger GOx molecule coating the nanoparticle. These assignments also can be observed in Table 2.

## 3.3 Raman spectroscopy

For further confirm the linkage of GOx on the AuNPs' surface, a characterization by Raman spectroscopy was performed. Figure 3A shows the Raman spectra of PVP and AuNPs-PVP; the peaks at 1670 $cm^{-1}$, 1430 $cm^{-1}$, and 1235 $cm^{-1}$ correspond to the pyrrolidone ring of PVP; in contrast the AuNPs-PVP spectrum shows an increment of this band (between 1100 – 1750 $cm^{-1}$), which is attributed to stretching modes of the C=O bonds and the $CH_2$ bands of the PVP pyrrolidone ring (Luo et al., 2015) Figure 3B shows the Raman spectra of the GOx enzyme and the AuNPs-PVP-GOx nanocomplex. The following absorption bands of the GOx can be observed: at 1668 $cm^{-1}$ corresponding to amide I, 1610 $cm^{-1}$ for amide II, 1555 $cm^{-1}$ and 1460 $cm^{-1}$ for the C-H groups, 1273 $cm^{-1}$ for amide III, 1135 $cm^{-1}$ for the C-N groups, 855 and 846 $cm^{-1}$ for tyrosine, and 538 $cm^{-1}$ for S-S groups (Rygula et al., 2013). It is worth noting that this spectrum is complex due to the presence of a wide variety of functional groups; however, only some signals are observed and are poorly defined for the AuNPs-PVP-GOx. Figure 3C shows the evolution of Raman spectra after each functionalization stage; this figure shows that the AuNPs spectrum masks the PVP and GOx signals to a great extent. However, AuNPs functionalized with PVP and GOx showed a shift in the bands demonstrating their linkage with AuNPs. These assignments also can be observed in Table 3.

## 3.4 SEM characterization

Figure 4 shows micrographs of AuNPs, AuNPs-PVP, and AuNPs-PVP-GOx by SEM. The gold nanoparticles exhibited a uniform spherical morphology with a size of 16.58 ± 4.79 nm (Figure 4A); agglomeration of the NPs is observed in some regions. According to the elemental analysis by EDS, Al, C, O, Na, and Au signals can be observed. The main signal is Al, which comes from the substrate used to dry the samples. The C, O, and Na signals are related to the presence of citrate ions coming from the solution. The Au signal is due to the synthesized AuNPs. A spherical

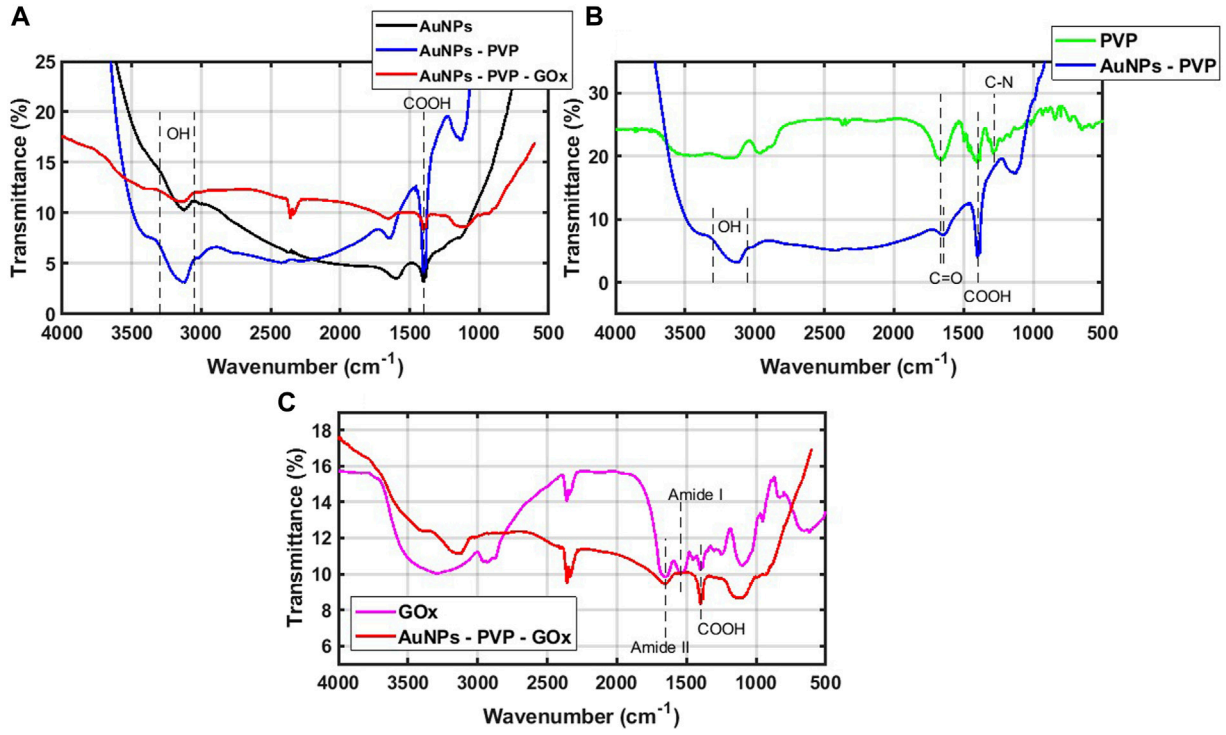


FIGURE 2
IR spectra **(A)** of AuNPs, AuNPs-PVP, and AuNPs-PVP-GOx. **(B)** Comparison of the IR spectra for PVP and AuNPs-PVP. **(C)** Comparison of the IR spectra for GOx and AuNPs-PVP-GOx.

TABLE 2 Assignments of the FTIR characterization bands of the solutions and nanoparticles used.

| PVP | | GOx | | AuNPs | |
|---|---|---|---|---|---|
| Wavenumber ($cm^{-1}$) | Assignment | Wavenumber ($cm^{-1}$) | Assignment | Wavenumber ($cm^{-1}$) | Assignment |
| 1291 | C-N bond | 1400 | Carboxyl groups | 3,125 | O-H bonds |
| 1400 | $CH_2$ group | 1539 | Amide I (N-H and C-H groups) | | (sodium citrate) |
| | | 1652 | Amide II (C=O) | | |

morphology is also evident in AuNPs-PVP; however, the particle size increased to 17.88 ± 6.94 nm (Figure 4B). In addition to the signals detected for AuNPs, the presence of nitrogen (N) was also recorded in the EDS spectrum, which is related to the adsorption of the pyrrolidone ring, in turn indicating that the polymer is linked to the nanoparticle.

In the case of the AuNPs-PVP-GOx, the same spherical morphology and particle size of 22.41 ± 5.19 nm were observed (Figure 4C). In this image, we presume that the light and dark areas are the GOx enzyme and the PVP, respectively; the bright spots correspond to the nanoparticles that are embedded in these nanocomplexes (Baruch-Shpigler and Avnir, 2022). As mentioned before, the presence of N is due to the enzyme and the PVP, while the Na and P signals are due to PBS. Similarly, the Au signal is associated with the synthesized nanoparticles. In general, these results allow us to further confirm the passive functionalization of the AuNPs with the PVP polymer and the GOx enzyme.

## 3.5 Thermogravimetry analysis

AuNPs and AuNPs functionalized with PVP and GOx were analyzed by TGA (Figure 5). A gradual weight loss is observed as the temperature increases from 30°C to 102°C (Phase I) for the three samples, which is due to a dehydration process. Subsequently, an additional weight loss is evident from 103°C to 107°C (Phase II), which is probably related to the loss of water adsorbed on the AuNPs. In the case of AuNPs-PVP and AuNPs-PVP-GOx, this water could be occluded in the polymer (PVP) and/or the enzyme (GOx), making difficult their expulsion from the nanocomplexes. At 107°C (Phase III), a total weight loss of water for AuNPs is observed; however, this phenomenon is different for AuNPs-PVP and AuNPs-PVP-GOx. It is important to note that the boiling temperature of PVP ranged from 90°C to 93 °C (O'Neil, 2001), thus it is likely to consider that PVP is decomposing at 107°C–124 °C. This weight loss pattern is similar for AuNPs-PVP-GOx, due to the evaporation of

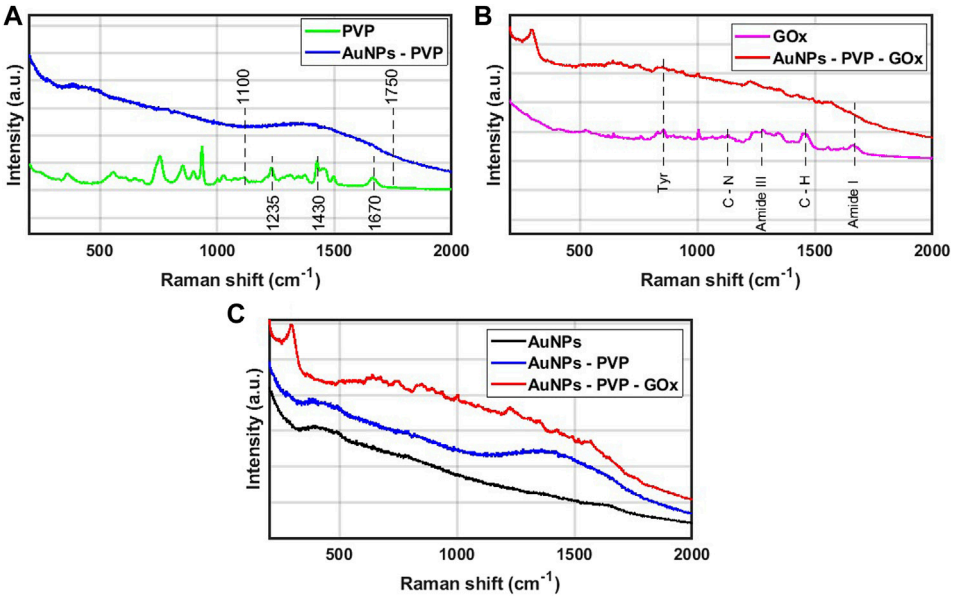


FIGURE 3
**(A)** Comparison of Raman spectra of PVP and AuNPs-PVP, **(B)** Comparison of Raman spectra of GOx and AuNPs-PVP-GOx, and **(C)** Raman spectra obtained for AuNPs, AuNPs-PVP and AuNPs-PVP-GOx samples.

TABLE 3 Assignments of Raman spectra characterization bands of the solutions and nanoparticles used.

| PVP | | GOx | |
|---|---|---|---|
| Wavenumber ($cm^{-1}$) | Assignment | Wavenumber ($cm^{-1}$) | Assignment |
| 1100-1750 | C=O bond | 538 | S-S group |
| | $CH_2$ group | 846 and 855<br>1135 | Tyrosine<br>C-N group |
| 1235<br>1430<br>1670 | Pyrrolidone ring | 1273<br>1460 and 1555<br>1610<br>1668 | Amide III<br>C-H group<br>Amide II<br>Amide I |

PVP, however, the GOx enzyme could be denatured at high temperatures, so the weight loss is higher than in the other samples and the weight remains constant even at 140°C (phase IV).

## 3.6 UV-visible analysis

The UV-Visible absorption spectra of naked-AuNPs and those functionalized with PVP and GOx are shown in Figure 6. The AuNPs (Figure 6, black line) showed a maximum absorbance band at 537 nm [47], which is characteristic of NPs with a diameter over 16 nm (Kimling et al., 2006; Benkovičová et al., 2013). In the case of AuNPs-PVP, the maximum absorbance was detected at 540 nm (Figure 6, blue line). This shift of the absorption band to a longer wavelength could be attributed to a change on the surface of the gold nanoparticles due to the coating formed by the PVP (Benkovičová et al., 2013) which have an approximate core diameter of 20 nm. Likewise, a similar displacement of the wavelength was observed for AuNPs-PVP-GOx, with maximum absorbance at 545 nm (Figure 6, red line). This effect also could be attributed to the coating of GOx over the PVP layer on the AuNPs' surface, and a change of the core diameter to 24 nm (Benkovičová et al., 2013).

At each functionalization stage, the surface plasmon resonance (SPR) band can be observed which is characteristic of gold nanoparticles and shifted to a longer wavelength as the size of the nanoparticle core increases (Benkovičová et al., 2013).

## 3.7 DLS and Z potential

The hydrodynamic diameter and Z potential were measured using the DLS technique; the corresponding results are shown in Table 4. In addition, the hydrodynamic diameter and Z potential measurements can be seen in Figure 7. The average diameter of the naked-AuNPs was 48.60 ± 4.58 nm and its *Z* potential was −17.65 ± 1.50 mV; this negative value is attributed mainly to the citrate ions remaining on the AuNPs' surface (Jameel, 2017; Li et al., 2017).

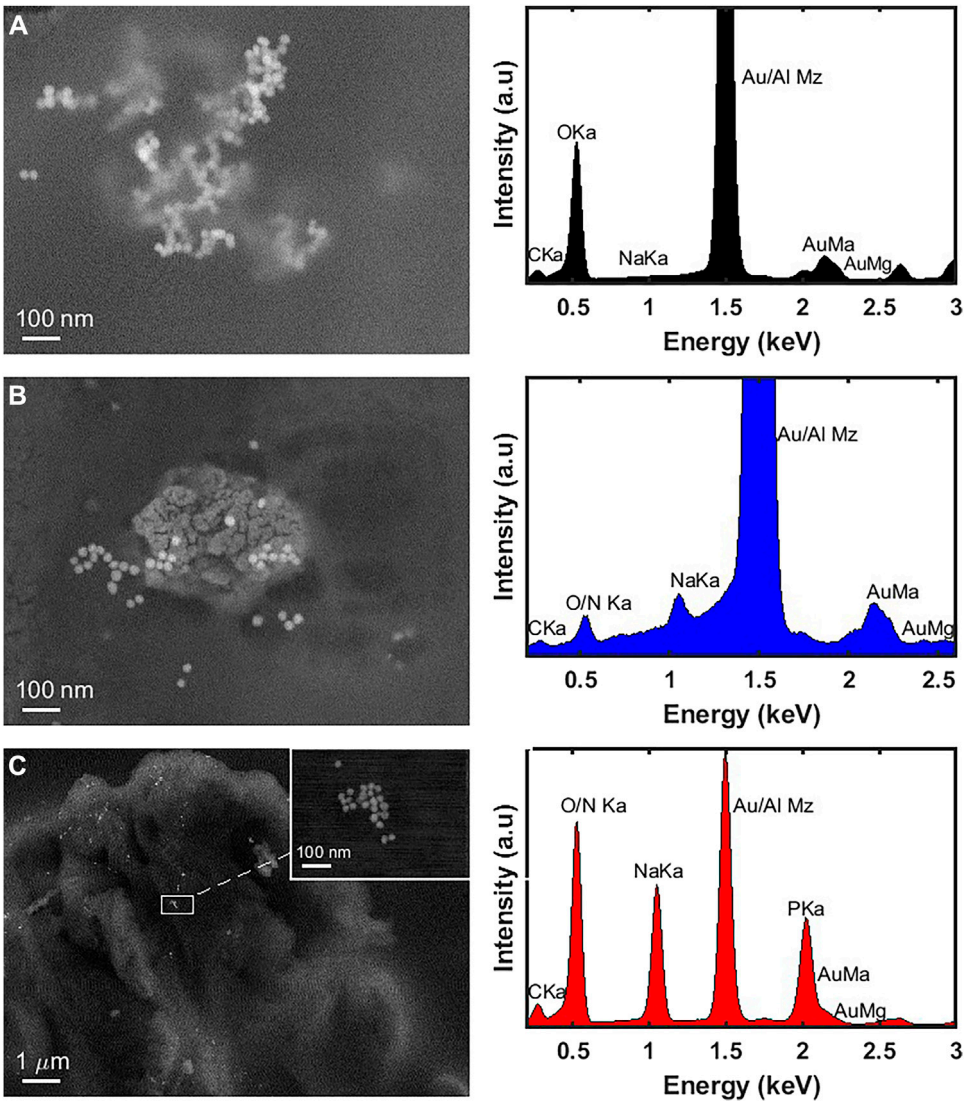


FIGURE 4
Scanning electron microscopy images and EDS analysis of **(A)** naked-AuNPs, **(B)** AuNPs-PVP, and **(C)** AuNPs-PVP-GOx.

The dynamic diameter increased to 150.37 ± 6.38 nm and the *Z* potential was −8.86 ± 4.64 mV for AuNPs-PVP, suggesting that the diameter increased because the carboxyl groups were blocked by PVP; notice that the polymer is coating the AuNPs surface (Rostek et al., 2011), which in turn produces a change on the surface potential compared to the AuNPs.

Similarly, an increase in the hydrodynamic diameter for AuNPs-PVP-GOx was detected, reaching 198.77 ± 24 nm, and the potential became more negative (−13.05 ± 0.74 mV). As indicated above, this increase was attributed to the passive binding of the amino groups of the GOx to the AuNPs' surface covered by PVP. In contrast, the change in potential is related to negatively charged species, mainly the R-groups of the active site such as His-516, His-559, and Glu-412 (Bauer JA et al., 2022). These results suggest that the gold nanoparticles were coated with PVP, favoring the adsorption of the enzyme and an increase of the hydrodynamic diameter as well as the change of *Z* potential.

It is important to mention, that one way to verify the aggregation of nanoparticles is through the UV-vis technique with the detection of surface plasmon resonance (SPR). In the case of gold nanoparticles superficially linked to some analyte, the color of the colloidal solution changes from red to blue (Mehtala et al., 2014; Montaño et al. , 2023), resulting in aggregation which is called plasmon coupling (Montaño et al., 2023). In this work, these optical changes were not reflected in the colloid systems (Figures 1, 6). Therefore, this is evidence that the values obtained by DLC are more related to passive functionalization than to the aggregation of the particles.

## 3.8 Colorimetric evaluation of GOx biological activity

A colorimetric assay was performed after each functionalization stage to verify the presence of GOx and evaluate its biological activity (Table 1). The products of the

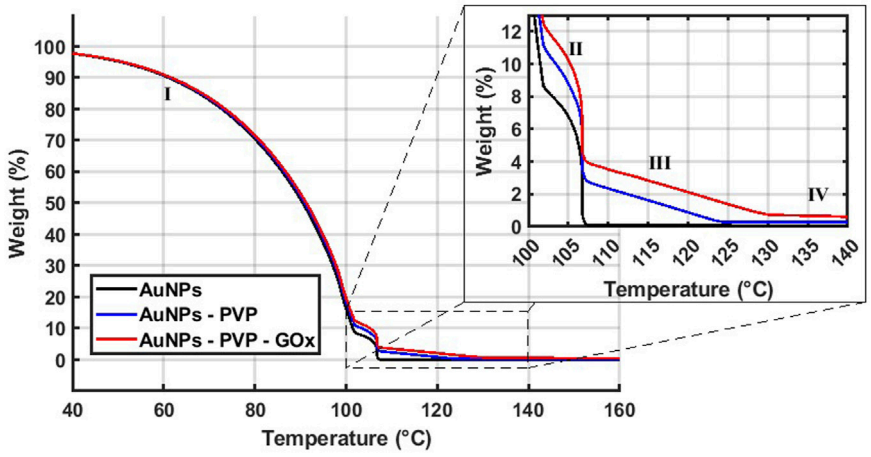


FIGURE 5
TGA curve of AuNPs, AuNPs-PVP, and AuNPs-PVP-GOx.

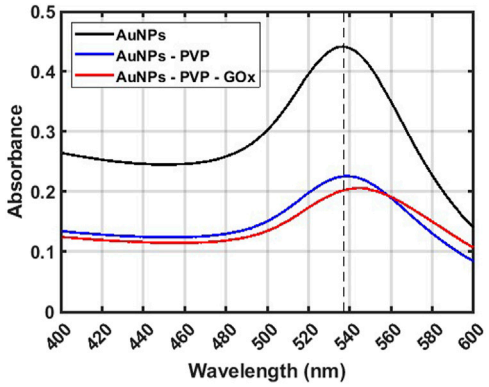


FIGURE 6
UV-Visible spectroscopy characterization.

enzymatic reactions for each sample are shown in Figure 8. Pure GOx was used as a positive control that produced a yellow color solution (Figure 8B), according to the reactions 1 and 2. In the presence of AuNPs-PVP-GOx a characteristic yellow coloration (Figure 8A) is observed, similar to that obtained in the presence of pure GOx (Figure 8B), supporting their biological activity and the functionalization of AuNPs with GOx. Conversely, there was no color change in the presence of AuNPs-PVP and AuNPs (Figures 8C,D, respectively) when they were exposed to a glucose standard; indicating that peroxide and triiodide ions were not formed.

## 3.9 Ultraviolet-visible absorption spectra analysis

As was mentioned above, the formation of peroxide and triiodide ions is expected from reaction 2; the formation of the triiodide ions $I_3^-$ can be detected by UV-Vis absorption spectra analysis. The reaction between hydrogen peroxide and potassium iodide was carried out for 5 min using different standards concentration. The UV-Visible characterization for each standard is shown in Figure 9A. In this figure, two absorption bands at 280 nm and 360 nm are observed reflecting the formation of triiodide ions; the appearance of these bands is related to $I_3^-$ electronic transitions (Guo et al., 2011). In addition, the absorbance increases as a function of the concentration of hydrogen peroxide, being proportional to the concentration of triiodide ions; therefore, an increase in absorbance is expected.

An absorbance calibration curve was constructed using data from Figure 9A. Figure 9B shows the absorbance (A) of the reaction in Eq. 2 as a function of hydrogen peroxide concentration $[H_2O_2]$ with an absorption band at 360 nm.

It is worth mentioning that a linear behavior is obtained at this range of concentrations; the equation of the linear fit is as follows:

$$A = 0.235[H_2O_2] + 0.354 \quad (3)$$

The correlation coefficient of the linear fit, r, was 0.9545; it was performed a hypothesis test to validate it through Student's t-test

TABLE 4 Average hydrodynamic diameter and *Z* potential of synthesized gold nanoparticles.

| Sample | Hydrodynamic diameter (nm) | *Z* Potential (mV) |
|---|---|---|
| AuNPs | 48.60 ± 4.58 | −17.65 ± 1.50 |
| AuNPs-PVP | 150.37 ± 6.38 | −8.86 ± 4.64 |
| AuNPs-PVP-GOx | 198.77 ± 24.00 | −13.05 ± 0.74 |

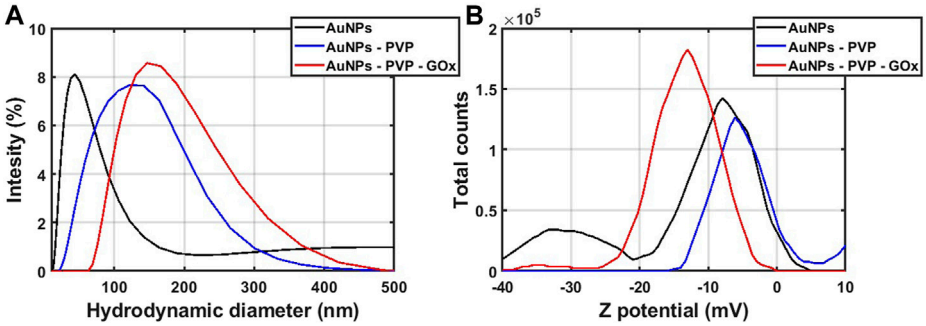


FIGURE 7
**(A)** Hydrodynamic diameter and **(B)** Z potential measurements of AuNPs, AuNPs-PVP, and AuNPs-PVP-GOx.

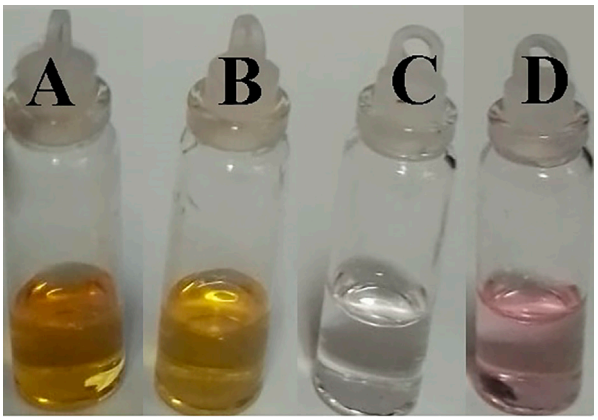


FIGURE 8
Enzymatic reactions of **(A)** AuNPs-PVP-GOx, **(B)** pure GOx (2,000 units) as a positive control, **(C)** AuNPs-PVP, and **(D)** naked-AuNPs.

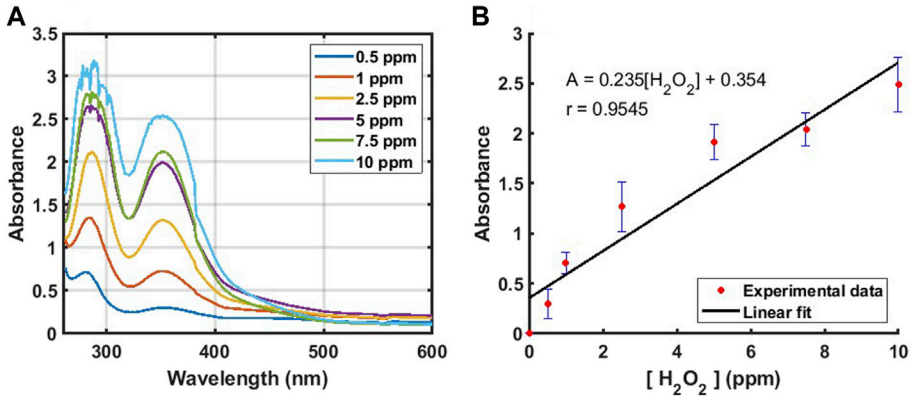


FIGURE 9
**(A)** UV-Vis absorption spectra of triiodide ions formed by reaction 2. **(B)** Absorbance vs. $[H_2O_2]$ plot at 360 nm.

(Mishra P et al., 2019) with a significance level of 0.05, and it was obtained that there was a significant correlation between absorbance and hydrogen peroxide concentration ($p = 1.72\,x10^{-11}$). This *p-value* guarantees that the experimental points present a linear trend that reliably correlates absorbance and hydrogen peroxide concentration.

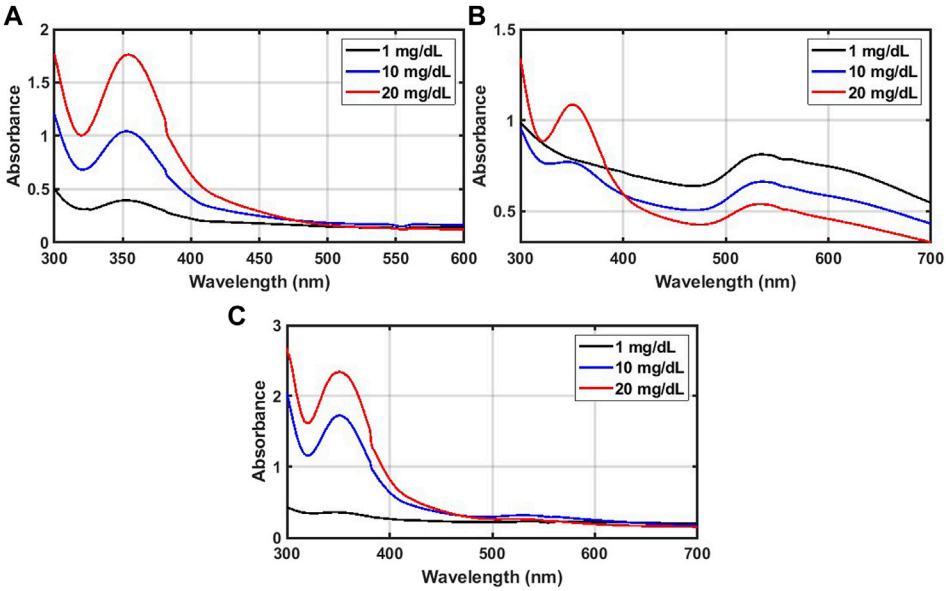


FIGURE 10
UV-Vis absorption spectra of solutions after enzymatic reaction with **(A)** GOX after 5 min, **(B)** AuNPs-PVP-GOx after 5 min, and **(C)** after 2.5 h.

## 3.10 Enzymatic assay with glucose oxidase and AuNPs-PVP-GOx

Three concentrations of D-glucose were prepared (1 mg/dL, 10 mg/dL, and 20 mg/dL) and the reaction (2) was carried out in the presence of GOx for 5 min. Then, the UV-vis characterization was recorded (Figure 10A). All the spectra show similar features, with a maximum absorption band at 360 nm, which is related to the formation of triiodide ions, as was described in the previous section. In addition, the absorption band increased as a function of the D-glucose concentration, which is in turn proportional to the hydrogen peroxide and triiodide ions formed during the reaction.

The same enzymatic reaction was then performed using AuNPs-PVP-GOx solution, without adding GOx; the resulting spectra are shown in Figure 10B (after 5 min) and 10c (after 2.5 h). In these figures, the spectra are similar to those obtained with pure GOx; the absorption band at 360 nm is evident and corresponds to the formation of the triiodide ions. In the presence of 1 mg/dL of D-glucose (Figure 10B), this absorption band is poorly defined, likely due to D-glucose's low concentration and/or the length of the reaction (time may not be enough for the formation of triiodide ions). In contrast, when the reaction time was 2.5 h (Figure 10C) the spectrum was well defined. In Figures 10B,C the maximum absorbance at 360 nm increased as a function of D-glucose concentration, with absorbance values better defined after 2.5 h of reaction, which indicates the formation of peroxide and triiodide ions. At 540 nm in the functionalized AuNPs (Figures 10B,C) correspond to the surface plasmon resonance band characteristic of gold nanoparticles. It seemed that during the formation of triiodide ions, the gold nanoparticles precipitated, as the absorbance at 540 nm decreased, especially after 2.5 h of reaction time. This means that the functionalized AuNPs can be used only as a transport vehicle of GOx.

Table 5 shows the average and standard deviation of hydrogen peroxide produced in three repetitions, according to Eq. 3. The quantity of peroxide generated was below 0.5 ppm in the presence of 1 mg/dL of D-glucose, which is due to its low concentration. With D-glucose at 10 mg/dL, a higher amount of peroxide was produced by GOx (2.75 ± 0.19 ppm), compared, to AuNPs-PVP-GOx (2.37 ± 0.63 ppm); this is because the concentration of GOx available in solution is greater than that on the nanoparticles. However, after 2.5 h of reaction, the amount of peroxide was 5.74 ± 0.28 ppm for the functionalized nanoparticles. This increment is due to the fact that a longer reaction time produces a greater amount of peroxide. Furthermore, these results were analyzed by Student's t-test with significance level of 0.05, and it was obtained that there is significant difference between two enzymatic reactions ($p = 5.11x10^{-5}$). It should be mentioned that the solution obtained from pure GOx after 2.5 h lost its initial color and became transparent; for this reason, this reaction time was not considered for the analysis.

Similarly, in the presence of 20 mg/dL of D-glucose, peroxide was obtained at 5.43 ± 0.37 ppm with GOx after 5 min; meanwhile, in the presence of AuNPs-PVP-GOx the peroxide concentration were 2.91 ± 0.17 ppm and 8.03 ± 0.39 ppm after 5 min and 2.5 h, respectively. The difference between these data was statistically significant according to Student's t-tests ($p = 5.42x10^{-4}$).

In addition, the limit of detection (LOD) of the sensor was calculated with the average value of the blank and 3.3 times the maximum standard deviation among all experimental data according to Yang et al. (Yang et al., 2019). The LOD of the developed sensor is 1 mg/dL and its linearity range is from 1 to 10 mg/dL.

## 3.11 Selectivity test

The reactions for selectivity test were carried out by the synthesized nanocomplexes in the presence of D-glucose, sucrose, mannose, agarose, and D-fructose for 5 min. The absorption spectra

TABLE 5 Hydrogen peroxide produced by enzymatic reaction with the different samples.

| D-glucose concentration (mg/dL) | $[H_2O_2]$ produced by GOx after 5 min (ppm) | $[H_2O_2]$ produced by AuNPs-PVP-GOx after 5 min (ppm) | $[H_2O_2]$ produced by AuNPs-PVP-GOx after 2.5 h (ppm) |
|---|---|---|---|
| 1 | <0.5 | <0.5 | <0.5 |
| 10 | 2.75 ± 0.19 | 2.37 ± 0.63 | 5.74 ± 0.28 |
| 20 | 5.43 ± 0.37 | 2.91 ± 0.17 | 8.03 ± 0.39 |

were obtained for each sample, and they are shown in Supplementary Figure S1. In the presence of glucose, as previously analyzed, the absorption band at 360 nm is observed, corresponding to the formation of triiodide ions, which is due to the oxidation of glucose by the nanocomplexes. However, for the other biomolecules, this absorption band was not observed, indicating that the enzymatic reaction between the GOx present in the nanocomplexes and these carbohydrates did not occur. For this reason, neither hydrogen peroxide nor triiodide ions were formed. These results demonstrate that the nanocomplexes (AuNPs-PVP-GOx) only react with glucose, showing their selectivity.

In addition, it is also important to note that the absorption bands due to the characteristic surface plasmon resonance of the gold nanoparticles can also be observed in the absorption spectrum. It is worth to mention that this selectivity test was conducted 1 year after the synthesis of the nanocomplex. Hence, the presence of the SPR in the absorption spectrum demonstrates that the nanoparticles remain stable even after being stored at 4°C for an extended period.

## 4 Discussion

In this work, the functionalization of AuNPs and GOx was achieved by passive adsorption using the PVP polymer as linkage. Although, PVP in AuNPs has already been used as a stabilizing agent (Mahato et al., 2019), it has not been used as a linkage on the surface of the AuNPs together with GOx. For instance, Amina et al. (Amina and Guo, 2020) report distinct types of linkage molecules on the surface of AuNPs; however, PVP was not used. Thus, the results presented in this work support the use of nanoparticles as biosensors for D-glucose.

Supplementary Table S1 shows the characteristic of some glucose biosensor and their detection methods. Although these systems show promising results, the methodologies used are complex and present certain disadvantages such as: risks of infection, weak absorption signals, interfering compounds, long detection time, among others (Peng et al., 2022). Our results showed that the enzymatic activity of GOx is preserved and even improved when it is linked to the surface of the AuNPs, which demonstrates a potential use of our nanocomplexes as D-glucose biosensors at low concentrations, such as those of different biological fluids (e.g., saliva) (Johnston L et al., 2021), in which the concentration of D-glucose is too low for detection through conventional glucose quantification methods (Pullano SA et al., 2022; Reddy et al., 2022). Furthermore, a high selectivity was determined for the synthesized nanocomplexes, since the AuNPs-PVP-GOx only reacted with D-glucose. This is a great advantage, since many types of carbohydrates can be present in many foods, and they can leave residues in saliva. However, it was demonstrated that with this method the presence of these biomolecules does not cause any interference for the glucose quantification.

In terms of the novelty of our work, it offers a glucose monitoring system for biofluids whose concentrations are lower compared to blood. This system presents an improvement in sensitivity and quantification of glucose from 1 mg/dL to 10 mg/dL compared to other methods described in the literature (please see Supplementary Table S1). It is worth to mention that this biosensor shows a detection time of 5 min; however, the signal is enhanced after 2.5 h. Moreover, this system will improve the disadvantages of commercial glucometers, such as eliminating finger pricks and providing a longer useful life. This was confirmed since the selectivity test was performed 1 year after synthesis, which suggest that the PVP coating provides great stability and fixation of the enzyme, so the functionalized NPs maintain the enzymatic activity after a long time. Finally, this system will also offer lower costs, since one of the advantages of the functionalization process is that it does not require many chemical reagents, making it a quick and economical process. An analysis of the cost of the reagents used and their quantities was performed; it was determined that the cost per test is approximately $1 USD.

Additionally, it is worth mentioning that the characterization techniques have not been used in previous studies (Li et al., 2007; Moses Phiri et al., 2019; Yang et al., 2019; Alshanberi et al., 2021), thus this information complements the study of AuNPs and their functionalization with GOx. The characterization techniques include a) the analysis of the change in the hydrodynamic diameter at larger sizes of the functionalized nanoparticles, relative to the naked nanoparticles using DLS; b) the analysis of change in the surface potential (Z potential), which demonstrated the stability on the nanocomplexes generated by PVP; c) Raman spectroscopy reveals the functionalization of AuNPs, which was indicated by bands corresponding to the pyrrolidone ring and amide groups on the surface of the nanocomplexes; d) the combination of SEM images and EDS analysis, indicates that GOx surrounds the nanoparticles together with the chemical elements; e) TGA revealing different phases of weight lost, due to the adhesion of PVP and GOx on the surface of the nanoparticles.

The timeline for using the developed biosensor involves the following steps: Extract 300 µL of saliva and add it to 300 µL of AuNPs-PVP-GOx, then read the absorption of the sample at 360 nm. Calculate the $H_2O_2$ concentration using Eq. 3, which is proportional to the D-glucose concentration in saliva, according to Table 5 it can be obtain:

$$[Glucose] = 4.3668\,[H_2O_2] - 15.0655 \quad (4)$$

Although it has been demonstrated that this test is reproducible, it may be necessary to recalibrate to ensure the accuracy of the relationship shown in Eq. 3.

## 5 Conclusion

The synthesis of gold nanoparticles was carried out using the Turkevich method. The functionalization of the AuNPs with PVP (AuNPs-PVP) and GOx (AuNPs-PVP-GOx) was carried out using a passive adsorption method and was characterized by UV-Visible, IR, Raman, Z potential, and TGA spectroscopy. After each functionalization step changes in the characterization were observed, including a shift in the SPR absorption band, an increase in the hydrodynamic diameter, a change in the Z potential, the detection of functional groups, and weight loss due to temperature increases. SEM/EDS microscopy also showed the size and morphology of the nanoparticles and the presence of chemical elements that indicate the presence of PVP and GOx. A colorimetric test was carried out to demonstrate the formation of peroxide and triiodide ions, also revealing the presence of GOx in the functionalized nanoparticles. Similarly, the formation of triiodide ions in the presence of GOx and AuNPs-PVP-GOx were determined using a calibration curve and hydrogen peroxide standards, and the selectivity test shown that this nanocomplex only react with D-glucose. These findings reveal the functionalization of AuNPs using PVP as a binding agent for GOx, which can be used in biosensor applications.

## Data availability statement

The raw data supporting the conclusions of this article will be made available by the authors, without undue reservation.

## Author contributions

IS-S: Methodology, Writing–original draft, Writing–review and editing. JZ-J: Formal Analysis, Software, Writing–original draft, Writing–review and editing. GV-M: Conceptualization, Methodology, Writing–original draft. RC-S: Conceptualization, Methodology, Supervision, Writing–review and editing. JB-L: Conceptualization, Supervision, Writing–review and editing.

## Funding

The author(s) declare that no financial support was received for the research, authorship, and/or publication of this article.

## Acknowledgments

The authors thank the Instituto Politécnico Nacional, the Secretaría de Investigación y Posgrado (SIP), and CONAHCYT for economic support for this work (Project No: 20231258). In addition, the authors are grateful to the members of the bioprocess laboratory, the polymer and nanomaterials research laboratory, the instrumental analysis laboratory, Centro Mexicano para la Producción más Limpia (CMPL), Centro de Nanociencias y Micro y Nanotecnologías (CNMN), CINVESTAV research laboratory, and the photothermal techniques laboratory for their support.

## Conflict of interest

The authors declare that the research was conducted in the absence of any commercial or financial relationships that could be construed as a potential conflict of interest.

## Publisher's note



## Supplementary material

The Supplementary Material for this article can be found online at: https://www.frontiersin.org/articles/10.3389/fnano.2024.1419239/full#supplementary-material

## References

Abdelghany, A. M., Meikhail, M. S., Oraby, A. H., and Aboelwafa, M. A. (2023). Experimental and DFT studies on the structural and optical properties of chitosan/polyvinyl pyrrolidone/ZnS nanocomposites. *Polym. Bull.* 80, 13279–13298. doi:10.1007/s00289-023-04700-0

Afrooz, M., and Dehghani, H. (2015). Effects of triphenyl phosphate as an inexpensive additive on the photovoltaic performance of dye-sensitized nanocrystalline TiO2 solar cells. *RSC Adv.* 5 (62), 50483–50493. doi:10.1039/c5ra06849e

Aldewachi, H., Chalati, T., Woodroofe, M. N., Bricklebank, N., Sharrack, B., and Gardiner, P. (2018). Gold nanoparticle-based colorimetric biosensors. *Nanoscale* 10 (1), 18–33. doi:10.1039/c7nr06367a

Alshanberi, A. M., Satar, R., and Ansari, S. A. (2021). Stabilization of β-galactosidase on modified gold nanoparticles: a preliminary biochemical study to obtain lactose-free dairy products for lactose-intolerant individuals. *Molecules* 26 (5), 1226. doi:10.3390/molecules26051226

Amina, S. J., and Guo, B. (2020). A review on the synthesis and functionalization of gold nanoparticles as a drug delivery vehicle. *Int. J. Nanomedicine* 15, 9823–9857. doi:10.2147/IJN.S279094

Arkaban, H., Barani, M., Akbarizadeh, M. R., Pal, S., Chauhan, N., Jadoun, S., et al. (2022). Polyacrylic acid nanoplatforms: antimicrobial, tissue engineering, and cancer theranostic applications. *Polym. (Basel)* 14 (6), 1259. PMID: 35335590; PMCID: PMC8948866. doi:10.3390/polym14061259

Bankar, S. B., Bule, M. V., Singhal, R. S., and Ananthanarayan, L. (2009). Glucose oxidase — an overview. *Biotechnol. Adv.* 27 (4), 489–501. doi:10.1016/j.biotechadv.2009.04.003

Bansal, S. A., Kumar, V., Karimi, J., Singh, A. P., and Kumar, S. (2020). Role of Gold nanoparticles in advanced biomedical applications. *Nanoscale Adv.* 2, 3764–3787. doi:10.1039/d0na00472c

Baruch-Shpigler, Y., and Avnir, D. (2022). Glucose oxidase converted into a general sugar-oxidase. *Sci. Rep.* 12, 10716. doi:10.1038/s41598-022-14957-6

Bauer, J. A., Zámocká, M., Majtán, J., and Bauerová-Hlinková, V. (2022). Glucose oxidase, an enzyme "ferrari": its structure, function, production and properties in the light of various industrial and biotechnological applications. *Biomolecules* 12 (3), 472. PMID: 35327664; PMCID: PMC8946809. doi:10.3390/biom12030472

Benkovičová, M., Végsö, K., Šiffalovič, P., Jergel, M., Majková, E., Luby, Š., et al. (2013). Preparation of sterically stabilized gold nanoparticles for plasmonic applications. *Chem. Pap.* 67 (9). doi:10.2478/s11696-013-0315-y

Chey, C., Ibupoto, Z., Khun, K., Nur, O., and Willander, M. (2012). Indirect determination of mercury ion by inhibition of a glucose biosensor based on ZnO nanorods. *Sensors* 12 (11), 15063–15077. doi:10.3390/s121115063

De Castro, L. F., de Freitas, S. V., Duarte, L. C., de Souza, J. A. C., Paixão, T. R. L. C., and Coltro, W. K. T. (2019). Salivary diagnostics on paper microfluidic devices and their use as wearable sensors for glucose monitoring. *Anal. Bioanal. Chem.* 411 (19), 4919–4928. doi:10.1007/s00216-019-01788-0

Dhumale, V. A., Gangwar, R. K., Datar, S. S., and Sharma, R. B. (2012). Reversible aggregation control of polyvinylpyrrolidone capped gold nanoparticles as a function of pH. *Mater. Express* 2 (4), 311–318. doi:10.1166/mex.2012.1082

Fahira, A. I., Amalia, R., Barliana, M. I., Gatera, V. A., and Abdulah, R. (2022). Polyethyleneimine (PEI) as a polymer-based Co-delivery system for breast cancer therapy. *Breast Cancer (Dove Med. Press)* 14, 71–83. PMID: 35422657; PMCID: PMC9005234. doi:10.2147/BCTT.S350403

Franco, P., and De Marco, I. (2020). The use of poly(N-vinyl pyrrolidone) in the delivery of drugs: a review. *Polymers* 12 (5), 1114. doi:10.3390/polym12051114

Goossens, J., Sein, H., Lu, S., Radwanska, M., Muyldermans, S., Sterckx, Y. G.-J., et al. (2017). Functionalization of gold nanoparticles with nanobodies through physical adsorption. *Anal. Methods* 9 (23), 3430–3440. doi:10.1039/c7ay00854f

Guo, F., Shi, L., and Wang, L. (2011). Experimental study of a closed system in the chlorine dioxide–iodine–ethyl acetoacetate–sulfuric acid oscillation reaction by UV-vis and online FTIR spectrophotometric methods. *J. Solut. Chem.* 40 (4), 587–607. doi:10.1007/s10953-011-9675-5

He, J., Xiao, G., Chen, X., Qiao, Y., Xu, D., and Lu, Z. (2019). A thermoresponsive microfluidic system integrating a shape memory polymer-modified textile and a paper-based colorimetric sensor for the detection of glucose in human sweat. *RSC Adv.* 9 (41), 23957–23963. doi:10.1039/c9ra02831e

Jameel, Z. N. (2017). Synthesis of the gold nanoparticles with novel shape via chemical process and evaluating the structural, morphological and optical properties. *Energy Procedia* 119, 236–241. doi:10.1016/j.egypro.2017.07.075

Johnston, L., Wang, G., Hu, K., Qian, C., and Liu, G. (2021). Advances in biosensors for continuous glucose monitoring towards wearables. *Front. Bioeng. Biotechnol.* 19 (9), 733810. PMID: 34490230; PMCID: PMC8416677. doi:10.3389/fbioe.2021.733810

Jung, D., Jung, D., and Kong, S. (2017). A lab-on-a-chip-based non-invasive optical sensor for measuring glucose in saliva. *Sensors* 17 (11), 2607. doi:10.3390/s17112607

Kimling, J., Maier, M., Okenve, B., Kotaidis, V., Ballot, H., and Plech, A. (2006). Turkevich method for gold nanoparticle synthesis revisited. *J. Phys. Chem. B* 110 (32), 15700–15707. doi:10.1021/jp061667w

Li, D., He, Q., Cui, Y., Duan, Li, and Junbai, Li (2007). Immobilization of glucose oxidase onto gold nanoparticles with enhanced thermostability. *Biochem. Biophys. Res. Commun.* 355 (2), 488–493. doi:10.1016/j.bbrc.2007.01.183

Li, N., Zang, H., Sun, H., Jiao, X., Wang, K., Liu, T. C.-Y., et al. (2019). A noninvasive accurate measurement of blood glucose levels with Raman spectroscopy of blood in microvessels. *Molecules* 24 (8), 1500. doi:10.3390/molecules24081500

Li, W., Shi, Z., Fang, C., Lu, Y., Yu, L., and Li, C. M. (2017). Integration of paper and micropipette tip to build a "sample-in, answer-out" point-of-care device. *Microfluid. Nanofluidics* 21 (4), 71. doi:10.1007/s10404-017-1901-z

Lipińska, W., Grochowska, K., and Siuzdak, K. (2021). Enzyme immobilization on gold nanoparticles for electrochemical glucose biosensors. *Nanomaterials* 11 (5), 1156. doi:10.3390/nano11051156

Liu, B., Zhang, J., and Guo, H. (2022). Research progress of polyvinyl alcohol water-resistant film materials. *Membr. (Basel)* 12 (3), 347. PMID: 35323822; PMCID: PMC8953738. doi:10.3390/membranes12030347

Luo, M., Hong, Y., Yao, W., Huang, C., Xu, Q., and Wu, Q. (2015). Facile removal of polyvinylpyrrolidone (PVP) adsorbates from Pt alloy nanoparticles. *J. Mater. Chem. A* 3 (6), 2770–2775. doi:10.1039/c4ta05250a

Mahato, K., Nagpal, S., Shah, M. A., Srivastava, A., Maurya, P. K., Roy, S., et al. (2019). Gold nanoparticle surface engineering strategies and their applications in biomedicine and diagnostics. *3 Biotech.* 9 (2), 57. doi:10.1007/s13205-019-1577-z

Mehtala, J. G., and Wei, A. (2014). Nanometric resolution in the hydrodynamic size analysis of ligand-stabilized gold nanorods. *Langmuir* 30 (46), 13737–13743. doi:10.1021/la502955h

Meyer, J. D., Manning, M. C., and Carpenter, J. F. (2004). Effects of potassium bromide disk formation on the infrared spectra of dried model proteins. *J. Pharm. Sci.* 93 (2), 496–506. doi:10.1002/jps.10562

Mishra, P., Singh, U., Pandey, C. M., Mishra, P., and Pandey, G. (2019). Application of student's t-test, analysis of variance, and covariance. *Ann. Card. Anaesth.* 22 (4), 407–411. PMID: 31621677; PMCID: PMC6813708. doi:10.4103/aca.ACA_94_19

Mohamed, T., Matou-Nasri, S., Farooq, A., Whitehead, D., and Azzawi, M. (2017). Polyvinylpyrrolidone-coated gold nanoparticles inhibit endothelial cell viability, proliferation, and ERK1/2 phosphorylation and reduce the magnitude of endothelial-independent dilator responses in isolated aortic vessels. *Int. J. Nanomedicine* 12, 8813–8830. doi:10.2147/ijn.s133093

Montaño Priede, J. L., Sanromán-Iglesias, M., Zabala, N., Grzelczak, M., and Aizpurua, J. (2023). Robust rules for optimal colorimetric sensing based on gold nanoparticle aggregation. *J. Am. Chem. Soc.* doi:10.1021/acssensors.3c00287

Moses Phiri, M., Wingrove Mulder, D., Mason, S., and Christiaan Vorster, B. (2019). Facile immobilization of glucose oxidase onto gold nanostars with enhanced binding affinity and optimal function. *R. Soc. Open Sci.* 6 (5), 190205. doi:10.1098/rsos.190205

Naresh, V., and Lee, N. (2021). A review on biosensors and recent development of nanostructured materials-enabled biosensors. *Sensors* 21 (4), 1109. doi:10.3390/s21041109

Nooranian, S., Mohammadinejad, A., Mohajeri, T., Aleyaghoob, G., and Kazemi Oskuee, R. (2021). Biosensors based on aptamer-conjugated gold nanoparticles: a review. *Biotechnol. Appl. Biochem.* 69, 1517–1534. doi:10.1002/bab.2224

Nukaly, H. Y., and Ansari, S. A. (2023). An insight into the physicochemical properties of gold nanoparticles in relation to their clinical and diagnostic applications. *Cureus* 15 (4), e37803. doi:10.7759/cureus.37803

M. J. O'Neil (2001). *The merck index - an encyclopedia of chemicals, drugs, and biologicals*. 13th Edition (Whitehouse Station, NJ: Merck and Co., Inc.), 1374.

Peng, Z., Xie, X., Tan, Q., Kang, Hu, Cui, Ji, Zhang, X., et al. (2022). Blood glucose sensors and recent advances: a review. *J. Innovative Opt. Health Sci.* 15. doi:10.1142/S1793545822300038

Pullano, S. A., Greco, M., Bianco, M. G., Foti, D., Brunetti, A., and Fiorillo, A. S. (2022). Glucose biosensors in clinical practice: principles, limits and perspectives of currently used devices. *Theranostics* 12 (2), 493–511. PMID: 34976197; PMCID: PMC8692922. doi:10.7150/thno.64035

Putzbach, W., and Ronkainen, N. (2013). Immobilization techniques in the fabrication of nanomaterial-based electrochemical biosensors: a review. *Sensors* 13 (4), 4811–4840. doi:10.3390/s130404811

Rachim, V. P., and Chung, W.-Y. (2019). Wearable-band type visible-near infrared optical biosensor for non-invasive blood glucose monitoring. *Sensors Actuators B Chem.* 286, 173–180. doi:10.1016/j.snb.2019.01.121

Reddy, V. S., Agarwal, B., Ye, Z., Zhang, C., Roy, K., Chinnappan, A., et al. (2022). Recent advancement in biofluid-based glucose sensors using invasive, minimally invasive, and non-invasive technologies: a review. *Nanomaterials* 12 (7), 1082. doi:10.3390/nano12071082

Rostek, A., Mahl, D., and Epple, M. (2011). Chemical composition of surface-functionalized gold nanoparticles. *J. Nanoparticle Res.* 13 (10), 4809–4814. doi:10.1007/s11051-011-0456-2

Rygula, A., Majzner, K., Marzec, K. M., Kaczor, A., Pilarczyk, M., and Baranska, M. (2013). Raman spectroscopy of proteins: a review. *J. Raman Spectrosc.* 44 (8), 1061–1076. doi:10.1002/jrs.4335

Sapountzi, E., Braiek, M., Vocanson, F., Chateaux, J.-F., Jaffrezic-Renault, N., and Lagarde, F. (2017). Gold nanoparticles assembly on electrospun poly(vinyl alcohol)/poly(ethyleneimine)/glucose oxidase nanofibers for ultrasensitive electrochemical glucose biosensing. *Sensors Actuators B Chem.* 238, 392–401. doi:10.1016/j.snb.2016.07.062

Sarfraz, N., and Khan, I. (2021). Plasmonic gold nanoparticles (AuNPs): properties, synthesis and their advanced energy, environmental and biomedical applications. *Chem. – Asian J.* 16 (7), 720–742. doi:10.1002/asia.202001202

Shahbazi, N., and Zare-Dorabei, R. (2019). A facile colorimetric and spectrophotometric method for sensitive determination of metformin in human serum based on citrate-capped gold nanoparticles: central composite design optimization. *ACS Omega* 4, 17519–17526. doi:10.1021/acsomega.9b02389

Shoaib, A., Ali, D., Khan, M. E., Azmi, L., Alalwan, A., Alamri, O., et al. (2023). A nanotechnology-based approach to biosensor application in current diabetes management practices. *Nanomaterials* 13 (5), 867. doi:10.3390/nano13050867

Si, P., Razmi, N., Nur, O., Solanki, S., Pandey, C. M., Gupta, R. K., et al. (2021). Gold nanomaterials for optical biosensing and bioimaging. *Nanoscale Adv.* 3 (10), 2679–2698. doi:10.1039/d0na00961j

Siripongpreda, T., Somchob, B., Rodthongkum, N., and Hoven, V. P. (2020). Bacterial cellulose-based re-swellable hydrogel: facile preparation and its potential application as colorimetric sensor of sweat pH and glucose. *Carbohydr. Polym.* 117506, 117506. doi:10.1016/j.carbpol.2020.117506

Teodorescu, M., and Bercea, M. (2015). Poly(vinylpyrrolidone) – a versatile polymer for biomedical and beyond medical applications. *Polymer-Plastics Technol. Eng.* 54 (9), 923–943. doi:10.1080/03602559.2014.979506

Xin Ting Zhao, V., It Wong, T., Ting Zheng, X., Nee Tan, Y., and Zhou, X. (2019). Colorimetric biosensors for point-of-care virus detections. *Mater. Sci. Energy Technol.* 3, 237–249. doi:10.1016/j.mset.2019.10.002

Xu, L., Chen, J., Ma, Q., Chao, D., Zhu, X., Liu, L., et al. (2022). Critical evaluation of the glucose oxidase-like activity of gold nanoparticles stabilized by different polymers. *Nano Res.* 16, 4758–4766. doi:10.1007/s12274-022-5218-1

Yamamoto, N., Kawashima, N., Kitazaki, T., Mori, K., Kang, H., Nishiyama, A., et al. (2018). Ultrasonic standing wave preparation of a liquid cell for glucose measurements in urine by midinfrared spectroscopy and potential application to smart toilets. *J. Biomed. Opt.* 23, 1. doi:10.1117/1.JBO.23.5.050503

Yang, Q. S., Zhang, X., Kumar, S., Singh, R. R., Zhang, B., Bai, C., et al. (2019). Development of glucose sensor using gold nanoparticles and glucose-oxidase functionalized tapered fiber structure. *Plasmonics* 15, 841–848. doi:10.1007/s11468-019-01104-7

Yeh, Y.-C., Creran, B., and Rotello, V. M. (2012). Gold nanoparticles: preparation, properties, and applications in bionanotechnology. *Nanoscale* 4 (6), 1871–1880. doi:10.1039/c1nr11188d

Yoo, E.-H., and Lee, S.-Y. (2010). Glucose biosensors: an overview of use in clinical practice. *Sensors* 10 (5), 4558–4576. doi:10.3390/s100504558

Zamora-Justo, J. A., Abrica-González, P., Vázquez-Martínez, G. R., Muñoz-Diosdado, A., Balderas-López, J. A., and Ibáñez-Hernández, M. (2019). Polyethylene glycol-coated gold nanoparticles as DNA and atorvastatin delivery systems and cytotoxicity evaluation. *J. Nanomater.* 2019, 1–11. doi:10.1155/2019/5982047

Zhang, J., Liu, J., Su, H., Sun, F., Lu, Z., and Su, A. (2021). A wearable self-powered biosensor system integrated with diaper for detecting the urine glucose of diabetic patients. *Sensors Actuators B Chem.* 341, 130046. doi:10.1016/j.snb.2021.130046

Zhou, T., Wang, M., He, X., and Qiao, J. (2019). Poly(vinyl alcohol)/Poly(diallyldimethylammonium chloride) anion-exchange membrane modified with multiwalled carbon nanotubes for alkaline fuel cells. *J. Materiomics* 5, 286–295. doi:10.1016/j.jmat.2019.01.012